Porous Materials

Highly Porous, Homochiral Metal–Organic Frameworks: Solvent-Exchange-Induced Single-Crystal to Single-Crystal Transformations**

*Chuan-De Wu and Wenbin Lin**

Porous metal–organic frameworks (MOFs) have recently received much attention owing to their potential applications in several technological areas such as gas storage, separation, and heterogeneous catalysis.[1] The modular nature of MOFs means they are readily tunable and, as a result, the synthesis of ideal, heterogenized single-site catalysts can be envisioned from porous MOFs by a judicious choice of metal-connecting nodes and/or bridging ligands.[2] Homochiral, porous MOFs are particularly attractive candidates as heterogeneous asymmetric catalysts for the economical production of optically active organic compounds due to the lack of chiral, inorganic zeolites.[3] Although we and others have recently provided preliminary evidence for the potential utility of homochiral, porous MOFs in enantioselective separation and catalysis,[4,5] several key issues remain to be addressed before practical applications of such materials can be realized. First, homochiral MOFs with permanent porosity are still extremely rare, even though there are now numerous reported examples of porous, achiral MOFs with extremely high surface areas.[6] Second, as yet there has been no study on the structural integrity of homochiral MOFs under catalytic conditions. Herein we report the design and synthesis of highly porous, homochiral solids based on 1D MOFs and their single-crystal to single-crystal transformations induced by solvent exchange. Our results suggest that the framework integrity of porous, homochiral MOFs can be maintained under typical asymmetric catalytic reaction conditions.

Colorless hexagonal crystals of $[CdL_2(ClO_4)_2]\cdot 11\,EtOH\cdot 6\,H_2O$ (**1**), where L is (*S*)-2,2′-diethoxy-1,1′-binaphthyl-6,6′-bis(4-vinylpyridine), were obtained by heating a mixture of $Cd(ClO_4)_2\cdot 6\,H_2O$ and L in DMF/*o*-$C_6H_4Cl_2$/EtOH at 70 °C for two days.[7] A single-crystal X-ray diffraction study revealed that **1** crystallizes in the chiral hexagonal space group $P6_222$ and adopts a 1D polymeric chain structure (Figure 1).[8] The adjacent Cd^{II} centers are linked by two L ligands to form 46-membered macrocycles with a Cd–Cd distance of 19.333(1) Å. The rhombic macrocycle has an opening of approximately 19.3×19.3 Å^2. Each

[*] Dr. C.-D. Wu, Prof. W. Lin
Department of Chemistry, CB#3290
University of North Carolina
Chapel Hill, NC 27599 (USA)
Fax: (+1) 919-962-2388
E-mail: wlin@unc.edu

[**] We acknowledge financial support from NSF. W.L. is an Alfred P. Sloan Fellow, an Arnold and Mabel Beckman Young Investigator, a Cottrell Scholar of Research Corp, and a Camille Dreyfus Teacher-Scholar.

Supporting information for this article is available on the WWW under http://www.angewandte.org or from the author.

  DOI: 10.1002/ange.200462711

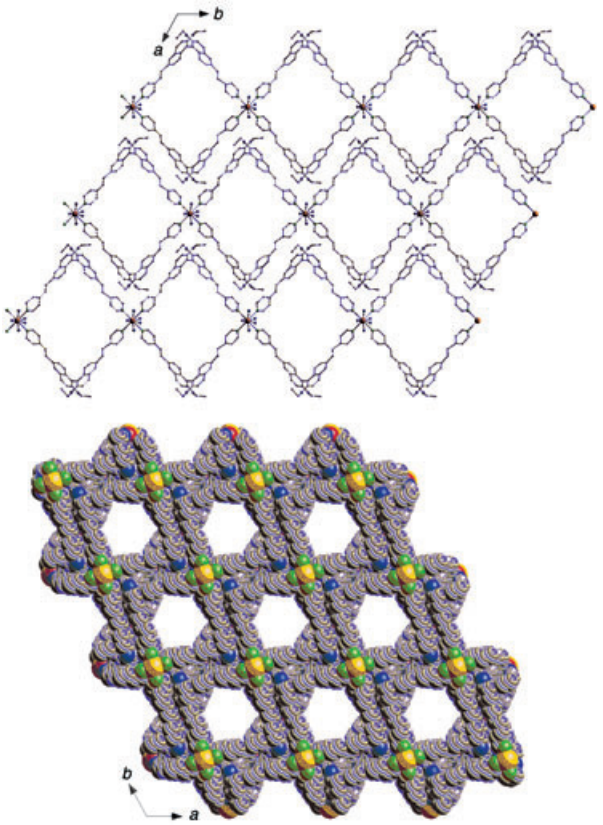

Figure 1. A view of the packing of the 1D polymeric chains in the *ab* plane (top) and a space-filling representation of **1** with chiral, 1D hexagonal channels (bottom).

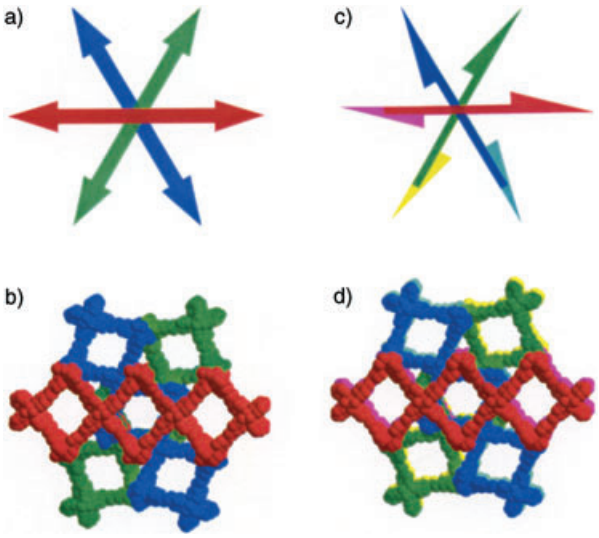

Figure 2. Schematic (a) and space-filling (b) views of the 6_2-helical arrangement of the 1D polymeric chains of **1** along the *c* axis. Schematic (c) and space-filling (d) views of the 6_1-helical arrangement of the 1D polymeric chains of **2a** along the *c* axis.

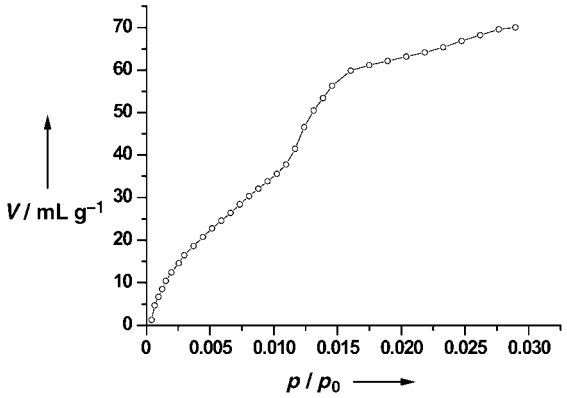

Figure 3. CO_2 gas-adsorption isotherm for an evacuated sample of **1** at 273 K.

Cd^{II} center adopts a slightly distorted octahedral environment by coordinating to four N atoms from four L ligands in the equatorial positions and two O atoms of two crystallographically disordered ClO_4^- ions in the axial positions. All the 1D chains lie parallel to each other in the *ab* plane due to interdigitation (Figure 1). These layer structures of **1** are stabilized by strong π···π stacking interactions (the nearest carbon-to-carbon separation is 3.360 Å between neighboring molecules). The 6_2 operation generates an …ABCABC… stacking pattern for all the 1D chains along the *c* axis, as shown in Figure 2. As expected, the 1D chains in the adjacent layers along the *c* axis are rotated by 120° with respect to each other to create chiral, 1D pseudo-hexagonal channels of 16.77 Å in dimension. There are no significant interactions between adjacent layers. Calculations with PLATON show that the effective volume for the inclusion is 4900.6 $Å^3$ per unit cell, which is 53.6% of the crystal volume.[9] TGA analysis indicated that a weight loss of 30.4% occurs between 20 and 194 °C, which corresponds to the loss of all the ethanol and water molecules (expected 30.4%).

We measured the CO_2 gas-sorption isotherm of **1** at 273 K to evaluate its permanent porosity. A sample of **1** was evacuated at 50 °C for 6 h under vacuum to remove the included solvent molecules before CO_2-adsorption measurements were attempted. As shown in Figure 3, a significant increase in the amount of CO_2 gas adsorbed by **1** was observed as the pressure of CO_2 increased, thus indicating the rapid diffusion of CO_2 molecules into the channels. The microporous surface area was calculated by fitting the adsorption data to the Dubinin–Radushkevich (DR) equation. The microporous surface area of an evacuated sample of **1** is 1096 $m^2 g^{-1}$, while the microporous volume is 0.47 $mL g^{-1}$. This level of porosity is among the highest reported for homochiral MOFs.

Whereas most applications of MOFs require only the presence of permanent porosity, the framework structures of homochiral MOFs need to be maintained in the presence of exchangeable solvents if they are to find applications in heterogeneous asymmetric catalysis. We therefore examined the framework stability of **1** during solvent removal and exchange processes. The X-ray diffraction pattern of **1** disappeared almost completely upon exposing the crystal to air for 30 min at room temperature. Such a distortion of the long-range order of homochiral MOFs upon solvent loss has

previously been observed in chiral, lamellar metal phosphonates.[10]

Interestingly, however, the X-ray diffraction patterns could be readily regenerated by submerging amorphous evacuated samples of **1** in either EtOH or benzene for 30 min. We also noticed that many crystals of **1** fractured into smaller pieces (while maintaining the same hexagonal morphology) after being submerged in EtOH or benzene for 30 min. In order to rule out the possibility that **1** may have undergone recrystallization due to the dissolution of the building blocks in EtOH or benzene, we carried out the solvent removal and exchange processes by exposing samples of **1** to air, EtOH vapor, or benzene vapor. After exposure of a crystal of **1** to benzene vapor for 12 h, no change in the morphology, size, or transparency of the crystal was observed under a microscope. An X-ray diffraction study, however, revealed that the benzene-exposed crystal (**2a**) has a formula of $[CdL_2(ClO_4)_2]\cdot 2\,C_6H_6\cdot 7\,EtOH\cdot 4\,H_2O$ as a result of the exchange of some of the ethanol and water guest molecules by benzene molecules. The unit-cell size of the crystal doubles as a result of the doubling of the *c*-axis in **2a**, and the space group of **2a** is $P6_122$ instead of $P6_222$ for **1** (Table 1). The most

Table 1: Selected crystallographic data for **1**, **2a**, **2b**, **3**, **2′**, and **1′**.

Compound	Space group	*a* [Å]	*c* [Å]	*V* [Å^3]	Solvent content[a]
1	$P6_222$	19.333	28.252	9145.1	$11\,EtOH\cdot 6\,H_2O$
2a	$P6_122$	19.442	55.939	18312.0	$2\,C_6H_6\cdot 7\,EtOH\cdot 4\,H_2O$
2b	$P6_122$	19.438	55.937	18304.3	$4\,C_6H_6\cdot 3\,EtOH\cdot 4\,H_2O$
3	$P6_222$	19.477	28.277	9289.8	$6\,C_6H_6\cdot H_2O$
2′	$P6_122$	19.431	55.968	18300.7	$2\,C_6H_6\cdot 7\,EtOH\cdot 2\,H_2O$
1′	$P6_222$	19.254	28.326	9094.2	$11\,EtOH\cdot 2\,H_2O$

[a] The solvent content is given per formula unit of $[CdL_2(ClO_4)_2]$.

significant structural difference between **1** and **2a** lies in the relative orientation of the ethoxy groups of the ligands L and the coordinating perchlorate groups, and the relative orientation of the 1D polymeric chains. As a result of these changes, the 1D polymeric chains stack in an …ABCDEFABCDEF… pattern along the *c* axis in **2a** instead of the …ABCABC… pattern in **1** (Figure 2). Unlike **1**, which has all the macrocycle planes parallel to the *ab* plane, the macrocycle planes in **2a** are slightly tilted away (by 0.2°) from the *ab* plane.[11]

Exposure of **2a** to benzene vapor for another 24 h caused more of the ethanol guest molecules to be replaced by benzene molecules, which results in a new crystal of the formula $[CdL_2(ClO_4)_2]\cdot 4\,C_6H_6\cdot 3\,EtOH\cdot 4\,H_2O$ (**2b**). Complex **2b** is structurally very similar to **2a** except that different numbers of solvent molecules are included. Further exposure of **2b** to benzene vapor resulted in complete replacement of EtOH by benzene to afford a new crystal of the formula $[CdL_2(ClO_4)_2]\cdot 6\,C_6H_6\cdot H_2O$ (**3**). Interestingly, the space group of the resulting crystal **3** is now $P6_222$ again and the packing of the 1D polymeric chains in **3** is essentially identical to that of **1**. The only difference between **1** and **3** lies in the inclusion of different solvent molecules. We also prepared samples of **3** by an entirely different route by slow diffusion of a solution of L in benzene into a solution of $Cd(ClO_4)_2$ in methanol.

Because the solvent-exchange processes are carried out in the presence of solvent vapors (with no condensed liquids), we believe that no dissolution of the MOFs occurs. The solvent exchange and accompanying structural transformation is thus a single-crystal to single-crystal process. Although several examples of single-crystal to single-crystal transformations were reported for achiral MOFs very recently,[12] this is the first example where chiral MOFs exhibit a single-crystal to single-crystal structural transformation induced by solvent exchange.

The structural transformation **1**⇔**2**⇔**3** is totally reversible. For example, a crystal of **3** can be transformed into **2′** and then **1′** by exposing **3** to ethanol vapor for varying amounts of time; the corresponding structures were verified by single-crystal X-diffraction studies. To eliminate the ambiguity of the solvent identities from X-ray diffraction studies, we also monitored the solvent-exchange processes by ^{1}H NMR spectroscopy. With an acetone internal standard and CD_2Cl_2 as the solvent, we determined that a freshly prepared sample of **1** contains 11 EtOH molecules per formula unit, which is consistent with the X-ray diffraction results (see Supporting Information). After exposure of **1** to benzene vapor for 12 h, crystals of **2** contain two benzene and 6.4 EtOH molecules, as determined by NMR integrations. Further exposure of **2** to benzene vapor for 48 h resulted in complete exchange of EtOH with benzene guest molecules. The reverse solvent-exchange processes **3**→**2′**→**1′** were also confirmed by ^{1}H NMR spectroscopy.

In summary, we have successfully constructed homochiral MOFs based on 1D polymeric chains. As schematically summarized in Figure 4, removal of the included solvent molecules from these MOFs leads to homchiral solids with permanent porosity and framework integrity. These homochiral MOFs undergo interesting reversible single-crystal to single-crystal structural transformations that are induced by solvent exchange. These results lend support to the notion that the framework structures of homochiral MOFs can be maintained during potential heterogeneous asymmetric catalytic reactions, and that true heterogeneous asymmetric catalysts can therefore be built from homochiral MOFs.

Experimental Section

1: A mixture of $Cd(ClO_4)_2\cdot 6\,H_2O$ (4.2 mg, 0.01 mmol), L (5.5 mg, 0.01 mmol), $CHCl_3$ (2 mL), *o*-$C_6H_4Cl_2$ (1 mL), and EtOH (1 mL) in a small, capped vial was heated at 70 °C for two days. Colorless crystals of **1** were isolated by filtration, washed with EtOH and Et_2O, and dried at room temperature. Yield: 5.8 mg (57.3% based on L). Elemental analysis (%) calcd. for **1**: C 58.2, H 7.07, N 2.77; found: C 60.4, H 4.24, N 3.43 (microanaylsis results are not informative owing to the ease of solvent loss). IR (KBr pellet): $\tilde{\nu}$ = 3462 (m), 3251 (w), 3085 (w), 2978 (w), 1605 (s), 1506 (m), 1468 (m), 1383 (w), 1327 (w), 1244 (m), 1203 (w), 1173 (w), 1108 (s), 1050 (m), 963 (w), 920 (w), 862 (w), 818 (w), 788 (w), 624 (m), 564 (w), 518 cm^{-1} (w).

NMR studies: A freshly prepared sample of **1** was exposed to benzene vapor. After 12 h, 13.2 mg of the benzene-exposed sample (**2**) was loaded into an NMR tube. A defined amount of acetone (ca. 1 μL) was added as the internal standard, followed by the solvent CD_2Cl_2. The absolute amounts of EtOH and benzene were deter-

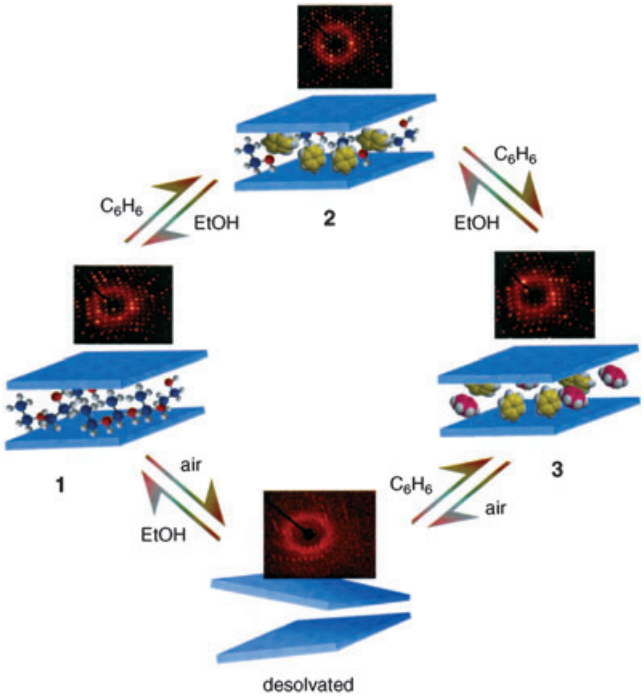

Figure 4. Schematic representation of the reversible single-crystal to single-crystal and single-crystal to amorphous to single-crystal transformation processes between **1**, **2**, and **3**.

mined by integration of the signature peaks. Similar NMR studies were carried out on **3** and samples of **1** and **2** that were prepared by exchanging the benzene guest molecules of **3**.

Received: November 24, 2004
Published online: February 23, 2005

Keywords: chirality · crystal engineering · functional materials · heterogeneous catalysis · metal–organic frameworks

[1] a) S. Kitagawa, R. Kitaura, S.-i. Noro, *Angew. Chem.* **2004**, *116*, 2388 – 2430; *Angew. Chem. Int. Ed.* **2004**, *43*, 2334 – 2375; b) B. Moulton, M. Zaworotko, *Chem. Rev.* **2001**, *101*, 1629 – 1658; c) M. Eddaoudi, D. B. Moler, H. Li, B. Chen, T. M. Reineke, M. O'Keeffe, O. M. Yaghi, *Acc. Chem. Res.* **2001**, *34*, 319 – 330; d) O. R. Evans, W. Lin, *Acc. Chem. Res.* **2002**, *35*, 511 – 522; e) N. G. Pschirer, D. M. Ciurtin, M. D. Smith, U. H. F. Bunz, H. C. zur Loye, *Angew. Chem.* **2002**, *114*, 603 – 605; *Angew. Chem. Int. Ed.* **2002**, *41*, 583 – 585; f) M. Fujita, Y. J. Kwon, S. Washizu, K. Ogura, *J. Am. Chem. Soc.* **1994**, *116*, 1151 – 1152.

[2] a) X. Zhao, B. Xiao, A. J. Fletcher, K. M. Thomas, D. Bradshaw, M. J. Rosseinsky, *Science* **2004**, *306*, 1012 – 1014; b) M. Oh, G. B. Carpenter, D. A. Sweigart, *Acc. Chem. Res.* **2004**, *37*, 1 – 11; c) G. S. Papaefstathiou, L. R. MacGillivray, *Coord. Chem. Rev.* **2003**, *246*, 169 – 184.

[3] B. Kesanli, W. Lin, *Coord. Chem. Rev.* **2003**, *246*, 305 – 326.

[4] a) J. S. Seo, D. Whang, H. Lee, S. I. Jun, J. Oh, Y. J. Jeon, K. Kim, *Nature* **2000**, *404*, 982; b) A. Hu, H. L. Ngo, W. Lin, *J. Am. Chem. Soc.* **2003**, *125*, 11490 – 11491; c) A. Hu, H. L. Ngo, W. Lin, *Angew. Chem.* **2003**, *115*, 6182 – 6185; *Angew. Chem. Int. Ed.* **2003**, *42*, 6000 – 6003; d) D. Bradshaw, T. J. Prior, E. J. Cussen, J. B. Claridge, M. J. Rosseinsky, *J. Am. Chem. Soc.* **2003**, *125*, 6106 – 6114.

[5] Related chiral hydrogen-bonded networks have also been reported: a) R. Custelcean, M. D. Ward, *Angew. Chem.* **2002**, *114*, 1800 – 1804; *Angew. Chem. Int. Ed.* **2002**, *41*, 1724 – 1728; b) P. Grosshans, A. Jouaiti, V. Bulach, J.-M. Planeix, M. W. Hosseini, J.-F. Nicoud, *Chem. Commun.* **2003**, 1336 – 1337.

[6] a) H. K. Chae, D. Y. Siberio-Perez, J. Kim, Y. Go, M. Eddaoudi, A. J. Matzger, M. O'Keeffe, O. M. Yaghi, *Nature* **2004**, *427*, 523 – 527; b) S. L. James, *Chem. Soc. Rev.* **2003**, *32*, 276 – 288; c) C. Janiak, *Dalton Trans.* **2003**, 2781 – 2804.

[7] The synthesis of L has been reported previously: Y. Cui, S. J. Lee, W. Lin, *J. Am. Chem. Soc.* **2003**, *125*, 6014 – 6015.

[8] X-ray single-crystal diffraction data for all the samples were collected on a Siemens SMART CCD diffractometer at 173 K. The data sets were corrected with the SADABS program (G. M. Sheldrick, SADABS, Siemens Analytical X-ray Instrument Division, Madison, WI, **1995**). The structures were solved by direct methods, and refined by full-matrix least-squares methods with the SHELXTL-97 program package (G. M. Sheldrick, SHELXTL-97, Program for Structure Refinement, University of Göttingen, Göttingen (Germany), **1998**). Selected crystallographic data are listed in Table 1; additional crystal data are given here. **1**: $Z=3$, $\rho_{calcd}=1.10\ g\,cm^{-3}$, $\mu(Mo_{K\alpha})=0.288\ mm^{-1}$, $R1=0.128$, $wR2=0.321$, Flack parameter = 0.06(12) and GOF = 1.12. **2a**: $Z=6$, $\rho_{calcd}=1.07\ g\,cm^{-3}$, $\mu(Mo_{K\alpha})=0.282\ mm^{-1}$, $R1=0.182$, $wR2=0.425$, Flack parameter = 0.1(1) and GOF = 1.08. **2b**: $Z=6$, $\rho_{calcd}=1.05\ g\,cm^{-3}$, $\mu(Mo_{K\alpha})=0.279\ mm^{-1}$, $R1=0.191$, $wR2=0.453$, Flack parameter = 0.06(12) and GOF = 1.06. **3**: $Z=3$, $\rho_{calcd}=1.02\ g\,cm^{-3}$, $\mu(Mo_{K\alpha})=0.271\ mm^{-1}$, $R1=0.084$, $wR2=0.201$, Flack parameter = −0.01(6) and GOF = 1.08. **2′**: $Z=6$, $\rho_{calcd}=1.05\ g\,cm^{-3}$, $\mu(Mo_{K\alpha})=0.280\ mm^{-1}$, $R1=0.194$, $wR2=0.442$, Flack parameter = 0.04(12) and GOF = 1.12. **1′**: $Z=3$, $\rho_{calcd}=1.07\ g\,cm^{-3}$, $\mu(Mo_{K\alpha})=0.285\ mm^{-1}$, $R1=0.091$, $wR2=0.229$, Flack parameter = 0.05(8) and GOF = 1.17. The high $R1$ values for **2a**, **2b**, and **2′** are probably a result of their metastable nature, which can lead to less perfect single crystals. CCDC-256708 (**1**), -256709 (**1′**), -256710 (**2′**), -256711 (**2a**), -256712 (**2b**), and -256713 (**3**) contain the supplementary crystallographic data for this paper. These data can be obtained free of charge from The Cambridge Crystallographic Data Centre via www.ccdc.cam.ac.uk/data_request/cif.

[9] A. L. Spek, *PLATON, A Multipurpose Crystallographic Tool*, Utrecht University, Utrecht, The Netherlands, **2001**.

[10] O. R. Evans, H. L. Ngo, W. Lin, *J. Am. Chem. Soc.* **2001**, *123*, 10395 – 10396.

[11] The macrocycle plane is defined by the Cd atoms and the middle of the 1,1′-carbon atoms of the binaphthyl moiety. **2b** and **2′** have a tilt angle of 0.2° and 1.1°, respectively.

[12] a) D. N. Dybtsev, H. Chun, K. Kim, *Angew. Chem.* **2004**, *116*, 5143 – 5146; *Angew. Chem. Int. Ed.* **2004**, *43*, 5033 – 5036; b) C. Y. Su, A. M. Goforth, M. D. Smith, P. J. Pellechia, H. C. zur Loye, *J. Am. Chem. Soc.* **2004**, *126*, 3576 – 3586; c) H. J. Choi, M. P. Suh, *J. Am. Chem. Soc.* **2004**, *126*, 15844 – 15851; d) R. Matsuda, R. Kitaura, S. Kitagawa, Y. Kubota, T. C. Kobayashi, S. Horike, M. Takata, *J. Am. Chem. Soc.* **2004**, *126*, 14063 – 14070; e) E. Y. Lee, M. P. Suh, *Angew. Chem.* **2004**, *116*, 2858 – 2861; *Angew. Chem. Int. Ed.* **2004**, *43*, 2798 – 2801.

